

Oxygen evolution in 30% KOH at 70°C on nickel anodically coated with CoOOH/Co₃O₄

L. BROSSARD

Institut de recherche d'Hydro-Québec, 1800 montée Ste-Julie, Varennes, Québec, Canada J3X 1S1

Received 21 December 1990

The oxygen evolution reaction (OER) was investigated on polished pure nickel electrodes preanodized for 30 min in nonpurified 30 wt % KOH at 70°C prior to determining the kinetic parameters of the OER. The electrolyte contained up to 0.8 mM dissolved cobalt and the preanodization current, i_a , ranged from 0.05 to 5 A cm⁻². In the presence of dissolved cobalt, an anodic coating of CoOOH/Co₃O₄ is formed on the nickel substrate. The electrocatalytic activity increases as i_a or the concentration in dissolved cobalt is increased. With 0.4 mM dissolved cobalt, the improved electrocatalytic activity is due to a linear increase in exchange current density through the charge associated with the reduction of the loading. The Tafel slope remains unaffected.

1. Introduction

One of the significant factors contributing to the lower performances of alkaline water electrolysis is the overpotential associated with the oxygen evolution reaction (OER) [1-3]. Nickel or nickel-based electrodes are considered attractive for the OER in the presence of hot concentrated alkaline solutions because nickel is relatively cheap, it is corrosion-resistant in the presence of concentrated KOH solutions and it has good electrocatalytic activity for the OER compared with those associated with expensive electrode materials.

The OER overpotential, η_{O_2} , can be significantly reduced by adding metallic species, e.g. Fe(II)/Fe(III) or Co(II) [4-6], to the concentrated KOH solution. The addition of cobalt (II) to a 30 wt % KOH at 90°C, resulting in the activation of nickel anodes during electrolysis at a current density of 1 A cm⁻², has been reported [6]: η_{O_2} is ~ 0.29 V after 200 h at 1 A cm⁻², η_{O_2} being stable with an anodic loading in cobalt of 4 mg cm⁻² or more. The authors postulate that cobalt is present mainly in the form of Co₃O₄ (spinel-type oxide) anodically deposited on the nickel substrate, while Co(II) is dissolved in the form of Co(OH)₄⁻² by adding cobalt nitrate to the caustic medium. No further information is given about either the amount of dissolved Co (II) in the electrolyte or the morphology of the coating and its influence on the kinetic parameters of the OER.

The present study investigates the activation of nickel anodes during electrolysis of 30 wt % KOH at 70°C in the presence of Co(III) species introduced by dissolving tris(ethylenediamine) Co(III) chloride hydrate. The concentration of Co(III) species was varied up to 0.8 mM. The nickel electrode was preanodized at a current density ranging from 0.05 to 5 A cm⁻² before measurement. Special attention was paid to the influence of the Co(III) concentration and,

in particular, to the preanodization current on the characteristics of the anodic deposit on the nickel substrate.

2. Experimental details

Cell preparation is described in detail elsewhere [7]. The working electrode consisted of a vertical 0.05 cm diameter nickel or cobalt wire (Met. Res. Corp. 99.99%) polished with alumina paste (1 μm).

The sample surface area was 0.157 cm². The temperature of the deaerated 30 wt % KOH aqueous solutions was maintained constant at 70°C by means of a Lauda M20 thermostatic bath.

The electrodes were preanodized for 30 min at an anodic current density (i_a) ranging from 0.05 to 5 A cm⁻². In some experiments, cobalt, in the form of tris(ethylenediamine) Co(III) chloride hydrate, was dissolved in the electrolyte; the Co(III) species ranged in concentration from 0.2 to 0.8 mM.

In a first set of experiments, the OER kinetic parameters were obtained after preanodization in the presence of either 0.4 mM dissolved cobalt with i_a ranging from 0.05 to 5 A cm⁻² or 0, 0.2, 0.6, and 0.8 mM dissolved cobalt with $i_a = 0.5$ A cm⁻². Immediately after preanodization, an anodic current of 0.052 A cm⁻² was applied for 1 min then decreased galvanostatically until a value of 1.1×10^{-4} A cm⁻² was reached. The Tafel parameters were determined from η_{O_2} corrected for the IR-drop.

In a second set of experiments, the nature of the accumulated oxides or hydroxides was investigated by cyclic voltammetry. Immediately after preanodization under experimental conditions similar to those associated with the first set of experiments, the electrode potential was varied in the cathodic direction at a scan rate of 0.1 V s⁻¹ and potentiodynamic traces were recorded.

The potentials were measured against a Hg/HgO/30 wt % KOH reference electrode at 70°C. The experimental value of the reversible potential for the hydrogen reaction in 30 wt % KOH at 70°C was -0.92 V with respect to this electrode, i.e. the reversible potential for the OER was $+0.278$ V.

The solutions were not purified prior to the experiments. The metallic impurities contained in the fresh 30 wt % KOH solutions were Al (2.5 p.p.m.), Pb (2.3 p.p.m.), Cr (1.3 p.p.m.), Ni (0.6 p.p.m.) and Fe (0.6 p.p.m.).

3. Results

3.1. OER

The oxygen overpotential, η_{O_2} (*IR*-corrected), is plotted against log current density in Fig. 1. The nickel (curve a) and cobalt (curve b) electrodes were preanodized with an electrolyte containing no dissolved cobalt (referred to below as NDC electrolyte) while in the case of curve c preanodization was carried out on a nickel substrate in the presence of 0.4 mM dissolved cobalt prior to the kinetic measurements. The preanodization time was 30 min and the current was 0.5 A cm^{-2} . With NDC electrolyte, it was noted that η_{O_2} is lower for cobalt than for nickel at any current density value. The exchange current density (i_0) and Tafel slope (b) are, respectively, $2.52 \times 10^{-7} \text{ A cm}^{-2}$ and 0.077 V dc^{-1} in the case of nickel (curve a) compared to $0.89 \times 10^{-7} \text{ A cm}^{-2}$ and 0.061 V dc^{-1} for cobalt (curve b).

The addition of 0.4 mM dissolved cobalt to the electrolyte resulted in a large decrease in η_{O_2} (curves a and c); for example, at 0.052 A cm^{-2} , η_{O_2} was 0.137 V lower. In the latter case (curve c), i_0 and b are, respectively, $29.4 \times 10^{-7} \text{ A cm}^{-2}$ and 0.064 V dc^{-1} . Consequently, b is practically the same for a cobalt electrode

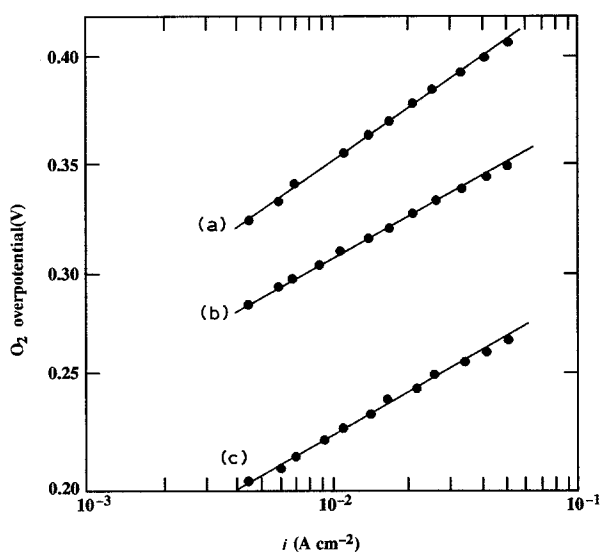


Fig. 1. Tafel lines for the OER after preanodization at 0.5 A cm^{-2} in 30 wt % KOH at 70°C. Preanodization time: 30 min; η_{O_2} values are *IR*-corrected. (a) Pure nickel substrate with no dissolved cobalt. (b) Pure cobalt substrate with no dissolved cobalt. (c) Pure nickel substrate in the presence of 0.4 mM dissolved cobalt.

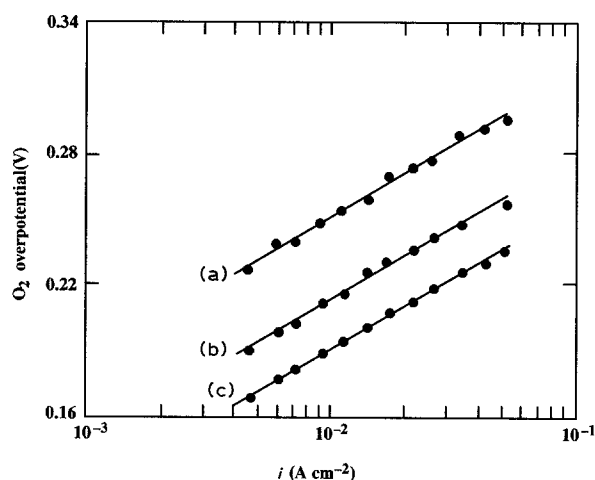


Fig. 2. Influence of preanodization current density on Tafel lines for nickel preanodized in the presence of 0.4 mM dissolved cobalt. Preanodization time: 30 min; η_{O_2} values are *IR*-corrected (30 wt % KOH, 70°C). Current density, i_a : (a) 0.05, (b) 1, (c) 5 A cm^{-2} .

preanodized with NDC electrolyte (curve b) as for a nickel electrode preanodized with dissolved cobalt (curve c).

The electrocatalytic activity of the nickel anode towards the OER also depends on the preanodization current, as illustrated in Fig. 2. In the presence of 0.4 mM dissolved cobalt, η_{O_2} at 0.052 A cm^{-2} shifts from 0.296 V for $i_a = 0.05 \text{ A cm}^{-2}$ to 0.235 V for $i_a = 5 \text{ A cm}^{-2}$. The kinetic parameters of the OER under the experimental conditions corresponding to Fig. 2 are summarized in Table 1 for i_a ranging from 0.05 to 5 A cm^{-2} . It is observed that b is practically constant with i_a ; consequently, the improvement in the electrocatalytic activity towards the OER with higher values of i_a is due to the increase in i_0 as i_a is shifted from 0.05 to 5 A cm^{-2} .

As shown in Fig. 3, the electrocatalytic activity of the nickel anode is influenced by the dissolved cobalt concentration in the electrolyte; for example, η_{O_2} at 0.052 A cm^{-2} is 0.282 V with 0.2 mM dissolved cobalt compared to 0.261 V with 0.8 mM dissolved cobalt. Preanodization was carried out at 0.5 A cm^{-2} for 30 min. The kinetic parameters of the OER are summarized in Table 2. It is observed that the influence of the Co(III) concentration on the kinetic parameters is small compared to the influence of the preanodization current (Table 1).

Table 1. Tafel parameters for the OER after preanodization at different current densities* in the presence of 0.4 mM Co

Preanodization current (A cm^{-2})	$i_0 \times 10^7$ (A cm^{-2})	b (V dc^{-1})
0.05	13	0.065
0.2	14	0.063
0.5	29	0.064
0.8	42	0.065
1	62	0.067
2	76	0.066
5	80	0.062

* 30 min preanodization in 30 wt % KOH at 70°C

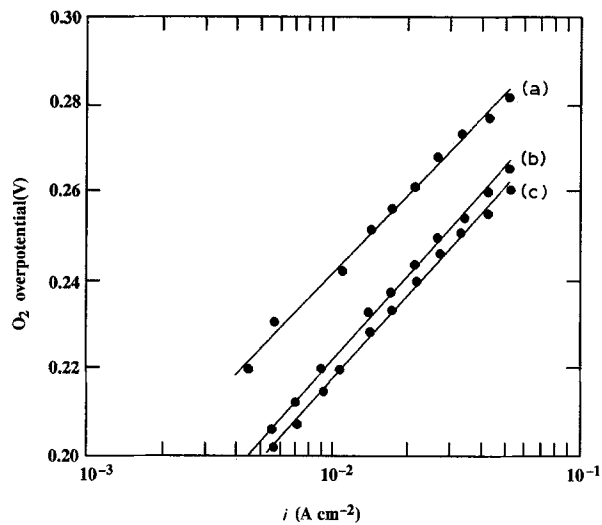


Fig. 3. Tafel lines after 30 min preanodization in the presence of different dissolved cobalt concentrations in 30 wt % KOH at 70°C. Preanodization time: 30 min and $i_a = 0.5 \text{ A cm}^{-2}$ for concentrations: (a) 0.2 (b) 0.6 and (c) 0.8 mM Co(III).

Table 2. Tafel parameters for the OER after preanodization* at 0.5 A cm^{-2} in the presence of dissolved cobalt

Concentration in dissolved cobalt (mM)	$i_0 \times 10^7 (\text{A cm}^{-2})$	$b (\text{V dc}^{-1})$
0.2	9.3	0.060
0.6	26	0.062
0.8	31	0.062

* 30 min preanodization in 30 wt % KOH at 70°C

3.2. Nickel surface after preanodization

SEM pictures of the nickel surface after preanodization at 0.05, 0.5 or 5 A cm^{-2} in the presence of 0.4 mM dissolved cobalt are given in Fig. 4. For $i_a = 0.05 \text{ A cm}^{-2}$, small nodules of a precipitate are observed on the nickel substrate (Fig. 4a). The nodule size and number per unit area increase as i_a is raised from 0.05 to

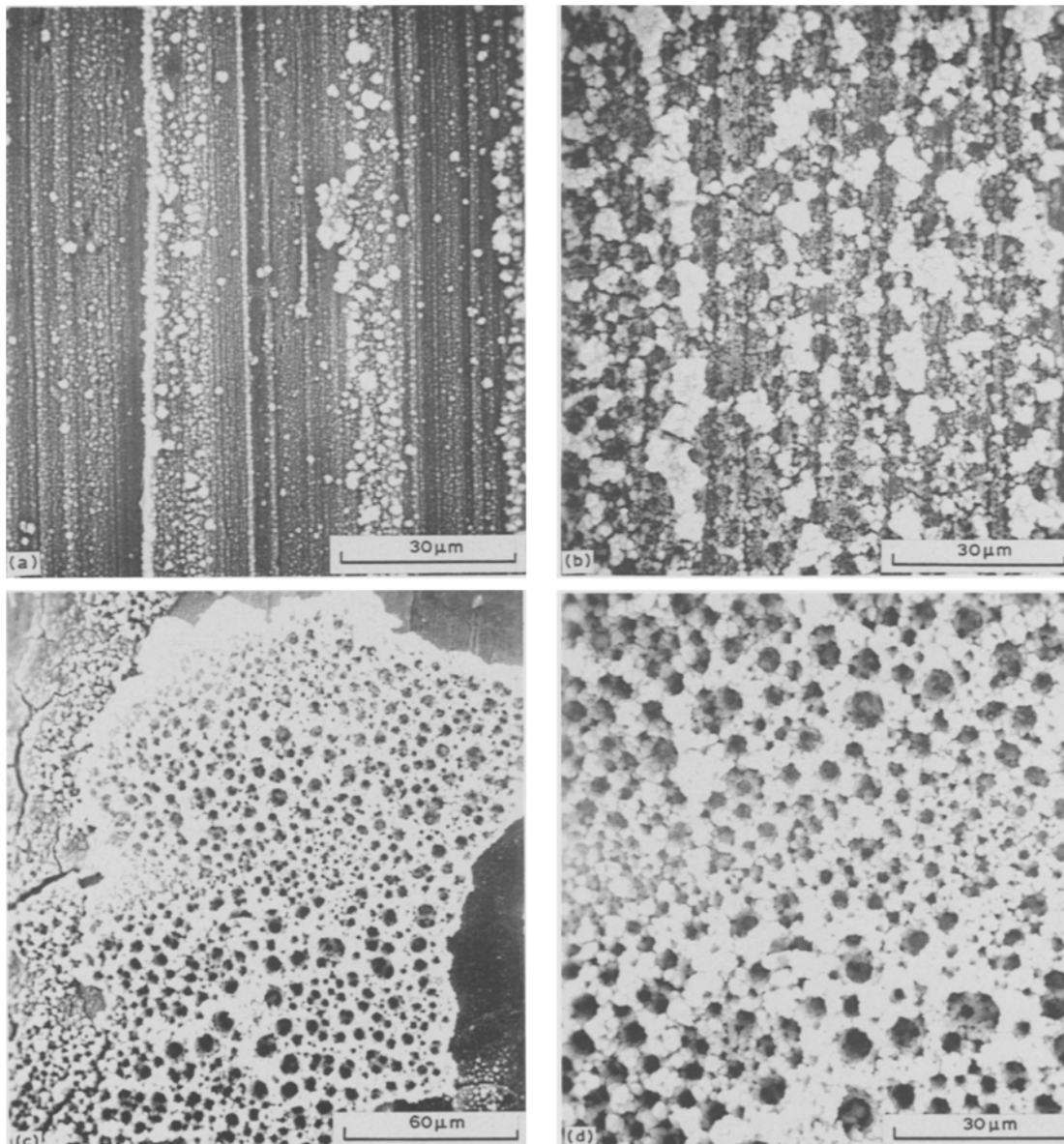


Fig. 4. Nickel surface after 30 min preanodization in the presence of 0.4 mM dissolved cobalt (30 wt % KOH, 70°C). Preanodization current: (a) 0.05; (b) 0.5; (c) 5 and also (d) 5 A cm^{-2} .

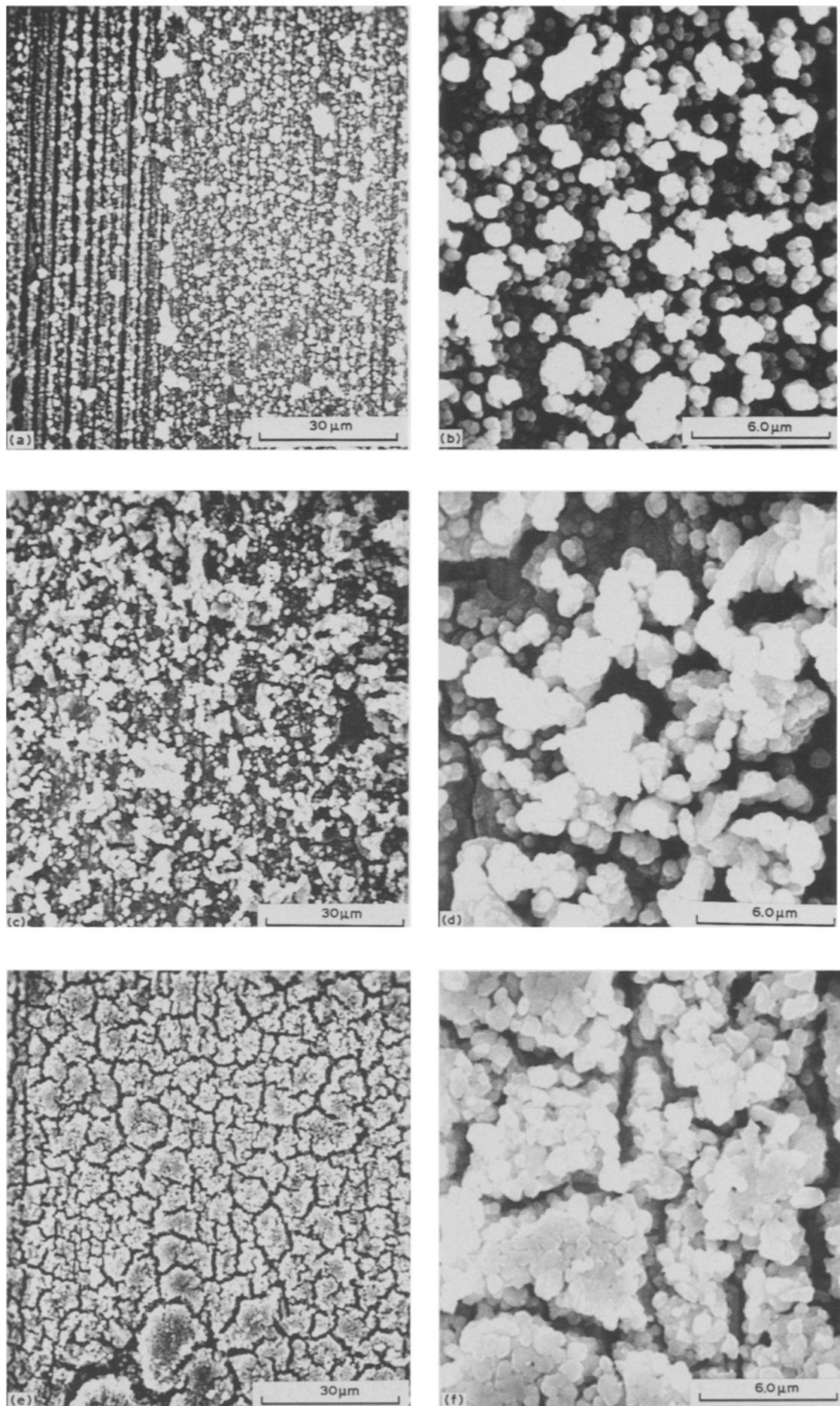


Fig. 5. Nickel surface after 30 min preanodization at 0.5 A cm^{-2} in the presence of dissolved cobalt (30 wt % KOH, 70°C). Concentration in dissolved cobalt: (a, b) 0.2, (c, d) 0.6 and (e, f) 0.8 mM Co.

0.5 A cm^{-2} (Fig. 4b). For $i_a = 5 \text{ A cm}^{-2}$, a coating containing cracks (Fig. 4c) and holes with a diameter ranging from 1 to $6 \mu\text{m}$ (Fig. 4d) is observed on the nickel surface.

The influence of the dissolved cobalt concentration on the morphology of the anodic deposit is illustrated in Fig. 5. The preanodization current is 0.5 A cm^{-2} for 30 min. The precipitate takes the form of large nodules, some with a diameter of several μm (Fig. 5a and b) when 0.2 mM Co(III) is dissolved in the electrolyte. From 0.2 mM Co(III) to 0.6 mM (III) , the amount of precipitate on the nickel electrode increases (Fig. 5c and d) while its morphology is practically unchanged; the main difference is that small cracks are present in the anodic coating with 0.6 mM Co(III) (Fig. 5d). The morphology of the anodic coating is different in the presence of 0.8 mM dissolved cobalt (Fig. 5e and f): nodules with a diameter of typically $0.7 \mu\text{m}$ are attached together and the coating is heavily cracked.

EDX analysis of surfaces corresponding to Figs 4 and 5 reveals that the anodic deposit contains cobalt. Elements with an atomic weight below 23 could not be detected with the probe available.

3.3. Nature of the deposit

The nature of the deposit on the electrode surfaces after preanodization was investigated by linear sweep voltammetry. Potentiodynamic traces were recorded after 30 min preanodization of a nickel wire electrode at $i_a = 0.05, 0.5$ or 5 A cm^{-2} in the NDC electrolyte in Fig. 6. Two reduction peaks, I and II, are present for $i_a = 0.5$ or 5 A cm^{-2} ; I is the dominant peak and is the only peak present for $i_a = 0.05 \text{ A cm}^{-2}$ (located at $\sim +0.30 \text{ V}_{\text{Hg/HgO}}$). The charges Q_I and Q_{II} related to peaks I and II are, respectively, 6.8 and 0 mC cm^{-2} for $i_a = 0.05 \text{ A cm}^{-2}$; 7.2 and 2.1 mC cm^{-2} for $i_a = 0.5 \text{ A cm}^{-2}$; and to 17 and 4.1 mC cm^{-2} for $i_a = 5 \text{ A cm}^{-2}$. Peak I is ascribed to the reduction of $\beta\text{-NiOOH}$ to Ni(OH)_2 on nickel [8] and, since it has no doublet, it is deduced that $\alpha\text{-NiOOH}$ is not present [9]. Peak II is attributed to the reduction of $\text{Ni}_3\text{O}_4(5)$, i.e. $\text{Ni}_3\text{O}_4 \rightarrow \text{Ni(OH)}_2$.

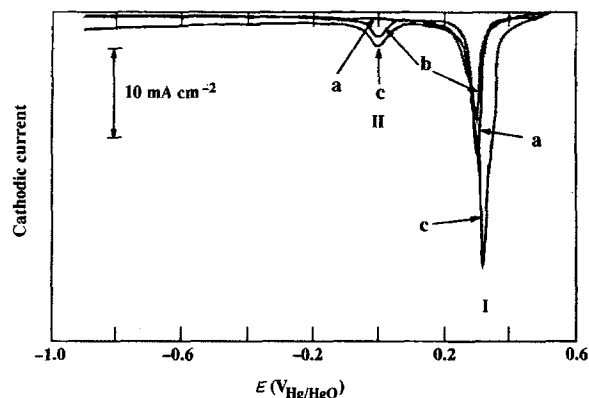


Fig. 6. Potentiodynamic traces after oxygen evolution on Ni in 30 wt % KOH at 70°C . Current densities, i_a (applied for 30 min): (a) 0.05 , (b) 0.5 and (c) 5 A cm^{-2} . Scan rate: 0.1 V s^{-1} was applied for 30 min.

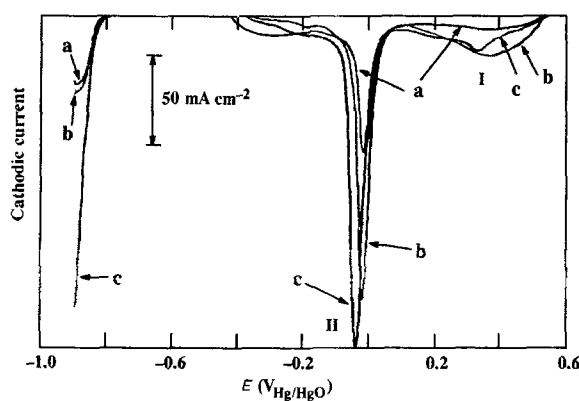


Fig. 7. Potentiodynamic traces after oxygen evolution on Co in 30 wt % KOH at 70°C . Current densities, i_a (applied for 30 min): (a) 0.05 , (b) 0.5 and (c) 5 A cm^{-2} . Scan rate: 0.1 V s^{-1} .

Potentiodynamic curves recorded after preanodization of cobalt at $i_a = 0.05, 0.5$ or 5 A cm^{-2} in the NDC electrolyte are presented in Fig. 7. Two reduction peaks are present, with peak I located at $\sim 0.32 \text{ V}_{\text{Hg/HgO}}$ and peak II at $\sim -0.02 \text{ V}_{\text{Hg/HgO}}$. Peak I is broad, while peak II is narrow and dominant. Peak I is probably due to the reduction of CoOOH to Co(OH)_2 and peak II to the reduction of Co_3O_4 to Co(OH)_2 [10, 11]. $Q_I = \sim 9 \text{ mC cm}^{-2}$ and $Q_{II} = \sim 32 \text{ mC cm}^{-2}$ for $i_a = 0.05 \text{ A cm}^{-2}$; $Q_I = \sim 49 \text{ mC cm}^{-2}$ and $Q_{II} = \sim 73 \text{ mC cm}^{-2}$ for $i_a = 0.5 \text{ A cm}^{-2}$ while $Q_I = \sim 41 \text{ mC cm}^{-2}$ and $Q_{II} = \sim 90 \text{ mC cm}^{-2}$ for $i_a = 5 \text{ A cm}^{-2}$.

Voltammograms of preanodized nickel in the presence of 0.4 mM dissolved cobalt in the electrolyte are given in Fig. 8. The preanodization time was 30 min and i_a ranged from 0.05 to 5 A cm^{-2} . A large broad peak (I) located at $\sim +0.3 \text{ V}_{\text{Hg/HgO}}$ is followed by a narrow peak (II) located at $-0.03\text{--}0 \text{ V}_{\text{Hg/HgO}}$.

The shape of the curves and the peak location are very similar in Figs 7 and 8 but in Fig. 8 a large increase in Q_I and Q_{II} is noted when i_a shifts from 0.05 to 5 A cm^{-2} . Q_I , Q_{II} and $Q_I + Q_{II} = Q_{\text{Tot}}$ are expressed against the preanodization current in Fig. 9. At any i_a value, $Q_{II} = \sim Q_I$ and Q_I , Q_{II} and Q_{Tot} increase almost linearly with i_a up to $\sim 1 \text{ A cm}^{-2}$.

The shape of the potentiodynamic traces and the location of the reduction peaks were similar to those

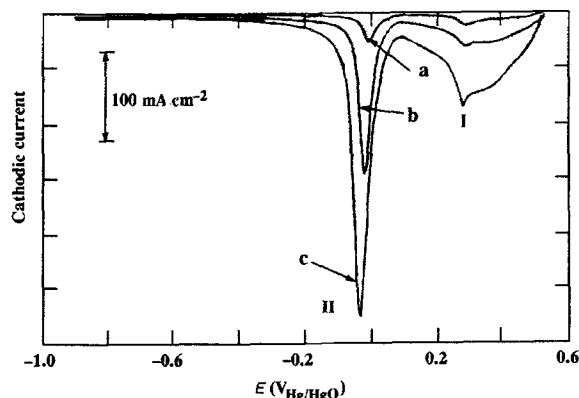


Fig. 8. Potentiodynamic traces after preanodization of nickel electrodes in the presence of 0.4 mM dissolved cobalt in 30 wt % KOH, 70°C . Current density, i_a : (a) 0.05 , (b) 0.5 and (c) 5 A cm^{-2} . Scan rate: 0.1 V s^{-1} .

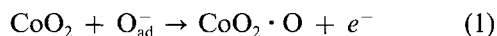
of Fig. 8 for dissolved cobalt concentrations of 0.2, 0.6 and 0.8 mM.

4. Discussion

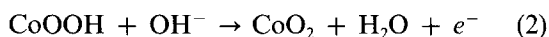
The kinetic parameters of the OER on preanodized nickel at $i_a = 0.44 \text{ A cm}^{-2}$ for 20 min in a nonpurified 30 wt % KOH at 70°C range from 0.064 to 0.077 V dc^{-1} for b and from 1.3×10^{-7} to $10 \times 10^{-7} \text{ A cm}^{-2}$ for i_0 [5]. These values are consistent with the values reported in the present investigation for nickel with $b = 0.077 \text{ V dc}^{-1}$ and $i_0 = 2.5 \times 10^{-7} \text{ A cm}^{-2}$ (curve a, Fig. 1). In the latter case, $i_a = 0.5 \text{ A cm}^{-2}$ and the preanodization time was 30 min, with no dissolved cobalt in the electrolyte.

With regard to the OER in a pre-electrolyzed KOH solution at 70°C , $b = 0.060 \text{ V dc}^{-1}$ and $i_0 = 1.0 \times 10^{-7} \text{ A cm}^{-2}$ for a cobalt electrode preanodized for 20 min at 0.44 A cm^{-2} [5]. These values are close to those reported in the present investigation for a preanodized cobalt electrode at $i_a = 0.5 \text{ A cm}^{-2}$, i.e. $b = 0.061 \text{ V dc}^{-1}$ and $i_0 = 0.89 \times 10^{-7} \text{ A cm}^{-2}$ (curve b, Fig. 1).

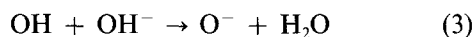
A Tafel slope $2/3$ (2.3) RFT^{-1} is compatible with two mechanisms [10, 11, 13]. The RDS of the first is:



and of the second:



A slope value of ~ 1 (2.3) RTF^{-1} is compatible with a mechanism [10] whose RDS is:



Since b is ~ 0.88 (2.3) RTF^{-1} in the present investigation (curve b, Fig. 1), it is deduced that the RDS corresponds mainly to Reaction 3.

For a nickel electrode preanodized in the presence of dissolved cobalt, from 0.2 to 0.8 mM Co(III), b varies from 0.86 to 1 (2.3) RTF^{-1} for i_a ranging from

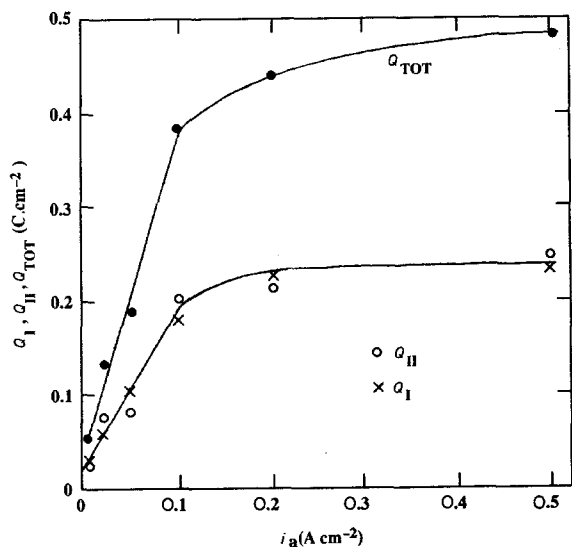


Fig. 9. Q_{I} , Q_{II} and $Q_{\text{I}} + Q_{\text{II}}$ against the preanodization current. The experimental conditions are those corresponding to Fig. 8.

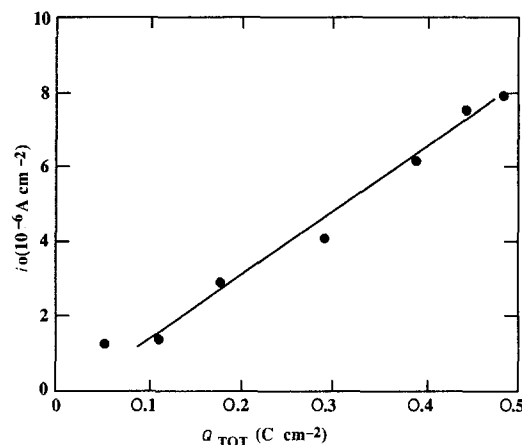


Fig. 10. The exchange current density (i_0) against the total charge of reduction obtained on potentiodynamic traces after preanodization of nickel electrodes in the presence of 0.4 mM dissolved cobalt. i_0 values are given in Table 1. Values of $Q_{\text{Tot}} = (Q_{\text{I}} + Q_{\text{II}})$ are given in Fig. 9.

0.05 to 5 A cm^{-2} (Fig. 2 and 3, Table 1). Consequently, it is deduced that the RDS of the OER also corresponds to Reaction 3.

The improvement in the electrocatalytic activity of a nickel electrode when the preanodization current is raised (Fig. 2 and Table 1) is related to the increase in i_0 with i_a when preanodization is done in the presence of 0.4 mM Co(III). This behavior is consistent with the accumulation of a porous anodic coating on the nickel surface (Fig. 4) while the amount of charge associated with the reduction of the coating, Q_{Tot} , increases significantly from 0.05 to 5 A cm^{-2} (Fig. 9). The values of i_0 in Table 1 are expressed against the total charge associated with the reduction in preanodized nickel in Fig. 10. The exchange current density increases linearly with a slope of $\sim 17 \times 10^{-6} \text{ A C}^{-1}$, as Q_{Tot} increases from 0.1 to 0.5 C cm^{-2} . This probably means that the interface for the OER increases linearly with the amount of anodic coating.

The anodic coating formed on nickel preanodized in the presence of dissolved cobalt is most likely a mixture of CoOOH and Co_3O_4 , since the coating contains cobalt. Furthermore, the shape of the potentiodynamic traces and the location of the reduction peaks are very similar for cobalt preanodized in the absence of dissolved cobalt (Fig. 7) and for nickel having an anodic coating (Fig. 8).

In addition, reduction for the same amount of cobalt for peaks I and II required 1 C for reducing CoOOH to $\text{Co}(\text{OH})_2$ (i.e. $\text{Co}(+3) \rightarrow \text{Co}(+2)$) compared to 0.67 C for reducing Co_3O_4 to $\text{Co}(\text{OH})_2$ (i.e. $\text{Co}(+2.67) \rightarrow \text{Co}(+2)$). Since $Q_{\text{II}} = \sim Q_{\text{I}}$ in Fig. 8, it can be concluded that, after preanodization in the presence of dissolved cobalt, the coating is CoOOH/ Co_3O_4 , the latter oxide being slightly dominant. For pure cobalt substrate preanodized in the absence of dissolved cobalt, the film is mainly Co_3O_4 , since $Q_{\text{I}} > Q_{\text{II}}$. Since the nature of the film is the same in both cases the Tafel slope is also practically the same.

The presence of cracks and holes in the coating (Figs 4 and 5) when the amount of the coating is large

enough is probably induced by the high oxygen flow rate during precipitation.

The influence of temperature on the nature and morphology of the anodic deposit and its electrocatalytic activity are under investigation.

References

- [1] C. T. Bowen, H. J. Davis, B. F. Henshaw, R. Lachance, R. L. Le Roy and R. Renaud, *Int. J. Hydrogen Energy* **9** (1984) 59.
- [2] L. Brossard, *ibid.* **13** (1988) 315.
- [3] D. E. Hall, *J. Electrochem. Soc.* **132** (1985) 41.
- [4] D. A. Corrigan, *ibid.* **134** (1987) 377.
- [5] L. Brossard, *Int. J. Hydrogen Energy* **16** (1991) 87.
- [6] H. Wendt, H. Hofmann and V. Plzak, *Mat. Chem & Phys.* **22** (1989) 27.
- [7] J. Y. Huot and L. Brossard, *Int. J. Hydrogen Energy* **12** (1987) 82.
- [8] P. W. T. Lu and S. Srinivasan, *J. Electrochem. Soc.* **125** (1978) 265.
- [9] F. Hahn, B. Beden, M. J. Croissant and C. Lamy, *Electrochim. Acta* **31** (1986) 335.
- [10] L. D. Burke, M. E. Lyons and O. J. Murphy, *J. Electroanal. Chem.* **132** (1982) 24.
- [11] T. R. Jayarama, V. K. Venkatesan and H. V. K. Udupa, *Electrochim. Acta* **20** (1975) 209.
- [12] H. Willems, A. G. C. Kobussen, J. H. W. De Wit and G. H. J. Broers, *J. Electroanal. Chem.* **17** (1984) 227.
- [13] P. Rasiyah, A. C. C. Tseung and D. B. Hibbert, *J. Electrochem. Soc.* **129** (1982) 1724.